Inorganic Chemistry

Communication

pubs.acs.org/IC

# Dynamic Entangled Framework Based on an Iridium–Organic Unit Showing Reversible Luminescence Turn-On Sensing

Lina Li,[†] Shuquan Zhang,[†] Yingying Xu,[†,‡] Sangen Zhao,[†] Zhihua Sun,[†] and Junhua Luo*[,†]

[†]Key Laboratory of Optoelectronic Materials Chemistry and Physics, Fujian Institute of Research on the Structure of Matter, Chinese Academy of Sciences, Fuzhou, Fujian 350002, China

[‡]University of the Chinese Academy of Sciences, Beijing 100039, China

Supporting Information

**ABSTRACT:** A new entangled metal–organic framework shows reversible structural dynamics and luminescence changing in response to the loss of guest $H_2O$ molecules. Furthermore, an intense and sensitive luminescence turn-on sensing was observed by the naked eye for **1** upon detection of the volatile organic solvent molecule $CH_3CN$, accompanied by reversible structural transformation.

Metal–organic frameworks (MOFs) are a class of materials that can be well-designed and contain active functional components with potential applications in catalysis, gas storage, chemical sensing, biomedical imaging, etc.[1] For chemical sensing, luminescent compounds act as highly sensitive and simple chemical sensors, which do not require extensive devices and can be detected by the naked eye. Luminescent MOFs are of great interest, are suitable for chemical sensing because of their tunable fluorescence, and have been widely studied in sensing ions,[2] gases,[3] solvents,[4] explosives,[5] etc. Dynamic MOFs are especially of interest because they readily undergo structural transformation that tends to enhance host–guest interaction, resulting in distinct luminescence signals.[6] The most common sensing in luminescent MOFs is quenching, or occasionally enhancement.[7] It is still less developed in sensing with luminescence shifts of MOFs upon analytes,[8] which is inherently more attractive than luminescence quenching (turn-off sensing). The analytes can be exactly read out, resulting from the appearance of a new shifted emission band (turn-on sensing). Thus, there is an urgent demand to develop luminescence turn-on sensing MOFs.

Iridium complexes,[9] with intense and tunable visible-light emission, are considered to be suitable for constructing MOFs with sensing properties. Our group recently reported an iridium-based MOF, which exhibits intense yellow-orange luminescence, providing us with a visual luminescence change in the detection of trace amounts of nitroaromatic explosives.[5b] In this paper, we report an iridium-based two-fold-entangled MOF, $[Zn(L)_2]\cdot 4H_2O$ [**1**; L = $Ir(ppy)_2(dcbpy)$, ppy = 2-phenylpyridine, and dcbpy = 2,2′-bipyridine-5,5′-dicarboxylate], which undergoes a dynamic structural transformation and shows discernible luminescence turn-on sensing on a volatile organic solvent, $CH_3CN$.

The iridium unit was prepared according to the literature[10] and reacted with $Zn(NO_3)_2\cdot 6H_2O$ in hydrothermal conditions to give red stick crystals of **1**, as shown in Figure S1 (detailed crystal data are given in Tables S1 and S2). Single-crystal X-ray analysis reveals that **1** crystallizes in tetragonal noncentrosymmetric space group $I4_1cd$ with a Flack parameter of 0.098(13). The three-dimensional (3D) framework of **1** is built from linking $Zn^{2+}$ metal centers with L bridging ligands. The asymmetric unit of **1** contains one L ligand and half of one $Zn^{2+}$ ion. As shown in Figure 1a, the independent $Zn^{2+}$ ion adopts a distorted

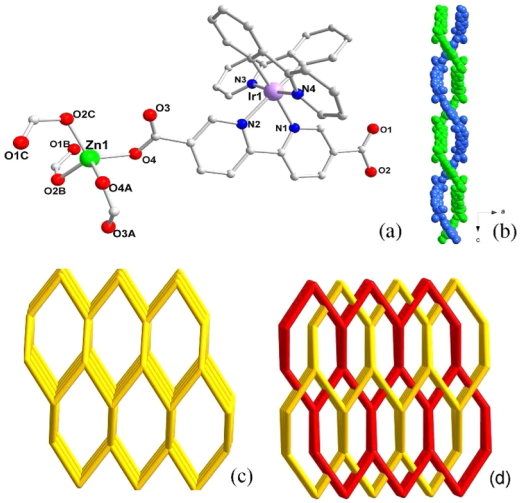


**Figure 1.** (a) Coordination environments of the $Zn^{II}$ ions. (b) Double-stranded helix chain in **1**. (c) Diamond topology framework for **1**. (d) 2-fold-entangled diamond topology framework for **1**. Symmetry codes: A, $1-x,-y,1-z$; B, $2-x,-y,1-z$; C, $x-1,y,z$ (H atoms are not shown for clarity).

tetrahedral coordination geometry and is coordinated by four carboxylate O atoms from four different L ligands [Zn–O distances range from 1.947(6) to 1.949(6) Å]. Notably, there is a double-stranded helical chain assembled by two left-handed helices in **1** along the *c* axis (Figure 1b), and the helical pitch is 49.069 Å. In addition, there are left- and right-handed helices constructed by the $Zn^{2+}$ ions and L ligands along the *b* axis (Figure S2a).

Considering each L ligand to be one connecting rod, an adamantine cage unit is formed by the link of $Zn^{2+}$ metal centers and L ligands, with the distance of adjacent $Zn^{2+}$ ions at

**Received:** March 26, 2015
**Published:** September 10, 2015





DOI: 10.1021/acs.inorgchem.5b00682
*Inorg. Chem.* 2015, 54, 8872–8874

14.9651(1) Å (Figure S2b). The 3D network of **1** is a diamond framework assembled by the cage units (Figure 1c). The framework with considerable void space readily accommodates a second framework via intergrowth, leading to a 2-fold-entangled structure for **1** (Figure 1d). Even with 2-fold entanglement, **1** exhibits large open channels that are filled with solvent molecules (Figure S2c). The $H_2O$ molecules lie in the void space. Such an entangled structural feature is favorable to producing structural transformation, as reported by others.[8b]

The powder X-ray diffraction (PXRD) patterns of the as-synthesized sample obtained match well with the simulated patterns, indicating that the compound is phase-pure (Figure S3). TGA data show that the guest $H_2O$ molecules are released in the temperature range of 35−135 °C and the dehydrated sample is stable up to 280 °C (Figure S4). Notably, reversible structural transformation was observed for **1** upon desolvation. The dehydrated sample **1a** was obtained by heating the as-synthesized sample at 100 °C in a vacuum oven for 3 h. The PXRD patterns of **1a** changed upon removal of the $H_2O$ molecules and then recovered to the original pattern of **1** after the sample was exposed to moisture in air (Figure S5), indicating that a distinct structural transformation occurs upon removal of the guest $H_2O$ molecules.

Interestingly, **1** exhibits a luminescence color change in response to the removal of $H_2O$ molecules, and the color tuning from red to orange can be distinguished by the naked eye. **1** displays a strong emission band at 620 nm excited at 500 nm visible light in the solid state (Figure S6), similar to that of the iridium unit with the maximum emission peak at 628 nm, indicating that the luminescence of **1** is generated by the iridium unit arising from metal-to-ligand charge transfer ($^3$MLCT). The luminescence decay is well fitted by a biexponential curve to give a lifetime of 6.8 $\mu$s for **1** (Figure S7). The desolvated sample **1a** exhibits orange luminescence at around 592 nm, which displays a distinct 28 nm blue shift from the red luminescence of **1** (Figure 2).

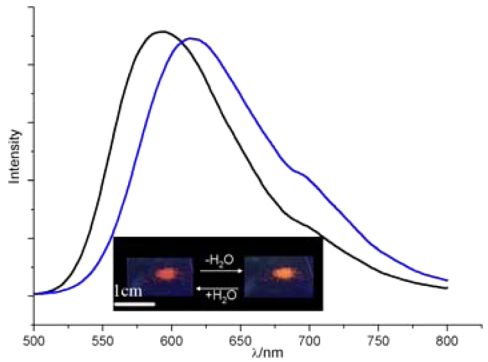


**Figure 2.** Solid-state emission spectra of **1** (blue) and **1a** (black). The inset photograph shows the reversible emission color change of **1** upon dehydration and rehydration under a UV lamp (365 nm).

The luminescence shift is attributed to changes in the energy levels of the iridium unit caused by enhancement in its secondary packing forces such as $\pi\cdots\pi$ and C−H$\cdots\pi$ interactions between the neighboring entangled frameworks upon structural transformation.[11] Remarkably, the luminescence emission returns to the original red emission of **1** when the sample was exposed to moisture in air.

Considering the dynamic structural transformation of **1**, we immersed the samples in several volatile organic solvents. As expected, **1** exhibited instant sensitivity to acetonitrile, with a visual color change from red to orange, while other solvents failed to induce evident color changes discerned by the naked eye (Figure S8), which agreed with the experimental luminescent spectra (Figure S9). In luminescence spectra, there was about a 30 nm blue shift of the emission band induced by acetonitrile. Moreover, the intensity of the maximum emission increased by 5 times that of the original sample under the same test conditions (Figure 3), and the quantum yield increased to 1.2% from 0.46%

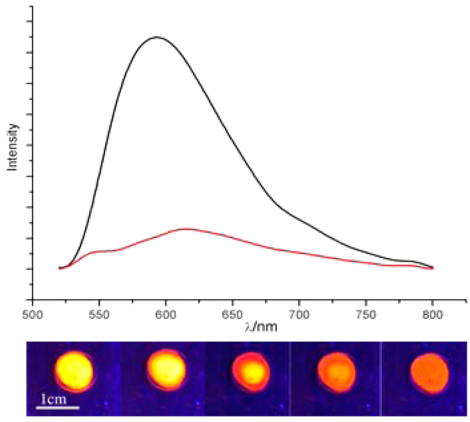


**Figure 3.** Top: Solid-state emission spectra of **1** with the $CH_3CN$ molecule (black) and **1** with $CH_3CN$ volatilization (red). Bottom: Luminescence change process of **1** with gradual $CH_3CN$ volatilization (from left to right).

(Figure S10). As a result, an obviously enhanced brightness was observed by the naked eye, featuring the rare luminescence turn-on sensing of the volatile $CH_3CN$ molecule. It was difficult to collect single-crystal data for **1** containing acetonitrile, so PXRD pattern changes were adopted to testify the structural transformation as reported by others.[4b,8c] Shifts of some peaks to lower angles were observed (Figure 4). The $^1$H NMR spectra

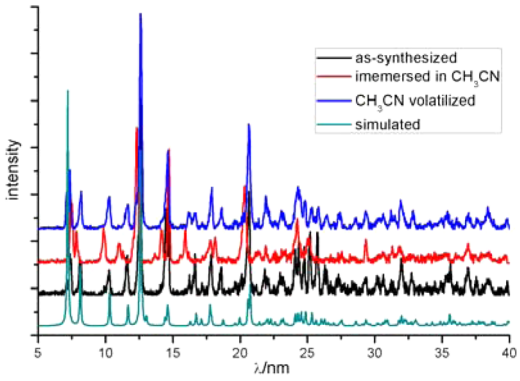


**Figure 4.** Simulated and experimental PXRD patterns of **1**.

testified the existence of $CH_3CN$ in **1** (Figure S11). Notably, after the acetonitrile-immersed sample was exposed to air, the luminescence immediately recovered to red via the release of acetonitrile molecules (Figure 3), accompanied by the structure recovered. The turn-on sensing signal is due to the fact that the triple bond in $CH_3CN$ molecules can affect the HOMOs and LUMOs of the iridium unit via intermolecular interaction, which provides efficient electron transfer to give rise to the enhanced emission,[12] and the dynamic structural transformation of the


DOI: 10.1021/acs.inorgchem.5b00682
*Inorg. Chem.* 2015, 54, 8872−8874

entangled framework strengthens the host−guest interactions.[8b,13]

In summary, an entangled MOF functionalized by embedding the iridium−organic unit has been synthesized. It shows reversible structural dynamics and luminescence change in response to the loss of guest $H_2O$ molecules. Moreover, an interesting luminescence turn-on sensing was observed by the naked eye for **1** upon detection of the volatile organic solvent molecule, $CH_3CN$. The dynamic structural transformation benefits the luminescence shift and turn-on sensing. This work will offer some insight into the structure−property relationships for the host−guest interaction responsive dynamics.

## ■ ASSOCIATED CONTENT

### Supporting Information

The Supporting Information is available free of charge on the ACS Publications website at DOI: 10.1021/acs.inorgchem.5b00682.

Experimental details, TGA, PXRD, NMR, photoluminescence, and luminescent decay lifetimes of **1** (PDF)

X-ray crystallographic data in CIF format (CCDC 1033341) (CIF)

## ■ AUTHOR INFORMATION


### Corresponding Author

*E-mail: jhluo@fjirsm.ac.cn.


### Notes

The authors declare no competing financial interest.

## ■ ACKNOWLEDGMENTS

This work was supported by the NSFC (Grants 21222102, 21373220, 51402296, 21171166, and 21301172), the 973 Key Program of MOST (Grant 2011CB935904), and the NSF of Fujian Province (Grant 2015J05040). L.L. thanks the "Youth Innovation Promotion Association CAS".

## ■ REFERENCES


(1) (a) Li, J.-R.; Sculley, J.; Zhou, H.-C. *Chem. Rev.* **2012**, *112*, 869−932. (b) Sumida, K.; Rogow, D. L.; Mason, J. A.; McDonald, T. M.; Bloch, E. D.; Herm, Z. R.; Bae, T.-H.; Long, J. R. *Chem. Rev.* **2012**, *112*, 724−781. (c) Kreno, L. E.; Leong, K.; Farha, O. K.; Allendorf, M.; Van Duyne, R. P.; Hupp, J. T. *Chem. Rev.* **2012**, *112*, 1105−1125. (d) Li, L. N.; Zhang, S. Q.; Xu, L. J.; Wang, J. Y.; Shi, L.-X.; Chen, Z.-N.; Luo, J. H.; Hong, M. C. *Chem. Sci.* **2014**, *5*, 3808−3813.

(2) (a) Que, E. L.; Domaille, D. W.; Chang, C. J. *Chem. Rev.* **2008**, *108*, 1517−1549. (b) Curiel, D.; Cowley, A.; Beer, P. D. *Chem. Commun.* **2005**, 236−238.

(3) Xie, Z.; Ma, L.; deKrafft, K. E.; Jin, A.; Lin, W. *J. Am. Chem. Soc.* **2010**, *132*, 922−923.

(4) (a) Lee, E. Y.; Jang, S. Y.; Suh, M. P. *J. Am. Chem. Soc.* **2005**, *127*, 6374−6381. (b) Stylianou, K. C.; Heck, R.; Chong, S. Y.; Bacsa, J.; Jones, J. T. A.; Khimyak, Y. Z.; Bradshaw, D.; Rosseinsky, M. J. *J. Am. Chem. Soc.* **2010**, *132*, 4119−4130.

(5) (a) Pramanik, S.; Zheng, C.; Zhang, X.; Emge, T. J.; Li, J. *J. Am. Chem. Soc.* **2011**, *133*, 4153−4155. (b) Li, L. N.; Zhang, S. Q.; Xu, L. J.; Han, L.; Chen, Z.-N.; Luo, J. H. *Inorg. Chem.* **2013**, *52*, 12323−12326.

(6) Manna, B.; Chaudhari, A. K.; Joarder, B.; Karmakar, A.; Ghosh, S. K. *Angew. Chem., Int. Ed.* **2013**, *52*, 998−1002.

(7) (a) Wang, C.; Lin, W. *J. Am. Chem. Soc.* **2011**, *133*, 4232−4235. (b) Fang, C.; Liu, Q.-H.; Ma, J.-P.; Dong, Y.-B. *Inorg. Chem.* **2012**, *51*, 3923−3925.

(8) (a) Zhang, M.; Feng, G. X.; Song, Z. G.; Zhou, Y.-P.; Chao, H.-Y.; Yuan, D. Q.; Tan, T. T. Y.; Guo, Z. G.; Hu, Z. G.; Tang, B. Z.; Liu, B.; Zhao, D. *J. Am. Chem. Soc.* **2014**, *136*, 7241−7244. (b) Takashima, Y.; Martínez, V. M.; Furukawa, S.; Kondo, M.; Shimomura, S.; Uehara, H.; Nakahama, M.; Sugimoto, K.; Kitagawa, S. *Nat. Commun.* **2011**, *2*, 168−175. (c) Jin, X. H.; Sun, J. K.; Cai, L. X.; Zhang, J. *Chem. Commun.* **2011**, *47*, 2667−2669.

(9) Zhao, Q.; Huang, C. H.; Li, F. Y. *Chem. Soc. Rev.* **2011**, *40*, 2508−2524. (b) Leung, C.-H.; Zhong, H.-J.; Yang, H.; Cheng, H.; Chan, D. S.-H.; Ma, V. P.-Y.; Abagyan, R.; Wong, C.-Y.; Ma, D.-L. *Angew. Chem., Int. Ed.* **2012**, *51*, 9010−9014. (c) Leung, C.-H.; Zhong, H.-J.; Chan, D. S.-H.; Ma, D.-L. *Coord. Chem. Rev.* **2013**, *257*, 1764−1776. (d) Man, B. Y.-W.; Chan, H.-M.; Leung, C.-H.; Chan, D. S.-H.; Bai, L.-P.; Jiang, Z.-H.; Li, H.-W.; Ma, D.-L. *Chem. Sci.* **2011**, *2*, 917−921. (e) Leung, K.-H.; He, H.-Z.; Ma, V. P.-Y.; Zhong, H.-J.; Chan, D. S.-H.; Zhou, J.; Mergny, J.-L.; Leung, C.-H.; Ma, D.-L. *Chem. Commun.* **2013**, *49*, 5630−5632.

(10) Jiang, W. L.; Gao, Y.; Sun, Y.; Ding, F.; Xu, Y.; Bian, Z. Q.; Li, F. Y.; Bian, J.; Huang, C. H. *Inorg. Chem.* **2010**, *49*, 3252−3260.

(11) Deshmukh, M. S.; Yadav, A.; Pant, R.; Boomishankar, R. *Inorg. Chem.* **2015**, *54*, 1337−1345.

(12) Liu, Z. W.; Bian, Z. Q.; Bian, J.; Li, Z. D.; Nie, D. B.; Huang, C. H. *Inorg. Chem.* **2008**, *47*, 8025−8030.

(13) Wang, J.-H.; Li, M.; Li, D. *Chem. Sci.* **2013**, *4*, 1793−1801.




DOI: 10.1021/acs.inorgchem.5b00682
*Inorg. Chem.* 2015, 54, 8872−8874